Realizing primary reference values in the nanoflow regime, a proof of principle

2010 Meas. Sci. Technol. 21 074003

(http://iopscience.iop.org/0957-0233/21/7/074003)

Meas. Sci. Technol. **21** (2010) 074003 (8pp) doi:10.1088/0957-0233/21/7/074003

Realizing primary reference values in the nanoflow regime, a proof of principle

Mijndert P van der Beek and Peter Lucas

VS, Department of R&D, PO Box 654, 2600 AR Delft, The Netherlands

E-mail: MvdBeek@VSL.nl

Received 25 November 2009, in final form 22 March 2010
Published 17 May 2010
Online at stacks.iop.org/MST/21/074003

Abstract
In this paper a proof of principle is demonstrated for a primary standard/nanoflow generator developed at the VSL (Van Swinden Laboratorium, The Netherlands). The ultimate goal of the research carried out at the VSL is to develop primary standards for liquid volume flows down to a few nanoliters per minute on the basis of sound traceability and low uncertainty. The nanoflow generator discussed in this paper is a first step in that direction and can generate flows in suction and discharge mode. The uncertainty of the generated flow is approximately 0.1% (2 s) relative at best. The flow generating process is based on the control of thermodynamic expansion of a driver liquid mass, whereas traceability is based upon volume transfer and conservation of mass (dynamic displacement principle).

Keywords: nanoflow, fluid flow generator, primary standard

(Some figures in this article are in colour only in the electronic version)

1. Introduction

Over the last decade, micro- and nanoflows have been appearing more frequently in various applications. For example, micro- and nanoflows appear in the fields of life science and technology [1], automotive [2], lab-on-a-chip, (near) vacuum metrology [3–6] and micro- and nanotechnology. Furthermore, micro/nanoflows appear more frequently in the medical world, for example in pain control pumps and possibly in under-the-skin implants for patient medicine supply in the near future. It is only a matter of time before other applications appear, and inherently the call for a sound traceability in the micro-nanoflow regime will emerge.

The ultimate goal with respect to a sound traceability is to have a primary standard to measure a certain fluid based on a single molecule counter (SMC). Although the realization of a SMC flowmeter is still beyond the horizon, progress is being made in the micro- and nanoflow regime. Recent research covers flowmeters and/or generators based on classic reciprocating displacement micro pumps, piezoelectrically driven reciprocating displacement micro pumps and dynamic micro pumps based on electromagnetic fields [7]. Furthermore, very small flow rates can be achieved with micro/nano dispensing based on the inkjet technology. In [1] a micro dispensing system is developed to be used in biotechnology which is able to dispense 50 μl volume samples with a covariance of 0.84 and 5 μl volume samples with a covariance of 2.7. Furthermore, in commercially available printers droplets of around 5 pl can be accurately created at frequencies ranging from 10 to 30 kHz [8]. However, these flowmeters/flowgenerators are not straightforward to use as a primary standard in the nanoflow regime. More importantly, these devices do not yet possess a sound traceability.

Therefore, the goal of the research carried out in the VSL (Van Swinden Laboratorium), Delft, The Netherlands, is to develop a relatively simple and straightforward primary standard/flowgenerator in the nanoflow regime with a sound traceability and low uncertainty. The goal of this paper is to demonstrate a proof of principle for a primary standard/nanoflow generator recently developed [9]. The principle of the primary standard/nanoflow generator is based upon the working principle of an ordinary liquid-in-glass thermometer. The difference from an ordinary thermometer is, however, a controlled temperature gradient which results in a *known* expansion of a liquid: the driving force for a fluid flow of interest (assuming that the 'thermometer' is open). The known volume rate can be used to calibrate very small flowmeters.

This paper is organized as follows. In section 2 we discuss the nanoflow generator. In this section we discuss

the working principle, a theoretical model and the realization of the prototype. In section 3 we discuss the uncertainty and rangeability of the nanoflow generator. Next, in section 4, we discuss the preliminary results achieved with the nanoflow generator which demonstrates the proof of principle. Finally, in section 5 the conclusions are drawn and future work is discussed.

2. Nanoflow generator

In this section the nanoflow generator developed at VSL is described in detail. In the following subsections, respectively, the working principle is explained, a basic theoretical framework is given and the realization of the prototype is discussed.

2.1. Working principle

The basis of the nanoflow generator is a very small capillary connected to a small reservoir of mercury, much like the conventional liquid-in-glass thermometers. The difference from an ordinary thermometer is that the capillary is open at the top side in order to create an outlet/inlet for the generated flow. The mercury, therefore, acts as a dynamic plunger to drive the fluid which is in contact with the mercury. In this proof of principle we will only consider the driving force (expansion of mercury) and not the volume rate of the fluid of interest (some liquid), which will be considered in future work. Figure 1 shows an illustration of the working principle of the nanoflow generator. The nanoflow generator is placed in an actively controlled thermodynamic water bath to control the temperature gradient and thus the flow rate.

The controlled thermodynamic water bath is placed in an another controlled temperature bath to minimize heat leakage. So far, the temperature in the water baths is controlled by adding a constant heat flux through an electric heating device, hence generating a constant temperature gradient. The linearity of the temperature change in time is not a strict prerequisite for getting a generated (traceable) reference volume; however, for the generation of a constant out- or inflow rate it is essential to have a constant temperature increase or decrease.

2.2. Basic theoretical model

Because the working principle of the nanoflow generator is nothing more than expansion of the mercury, we only need to be able to describe the volume of mercury as a function of time. The volume of the mercury is defined by

$$V(T) = \frac{m}{\rho(T)}, \tag{1}$$

where $V(T)$ is the volume as a function of the temperature T (in °C), m is the mass of the mercury (constant) and ρ is the density. The density of mercury for a given temperature is given by [10]

$$\rho(T) = \frac{\rho_{\mathrm{ref}}}{1 + A\,(T - T_{\mathrm{ref}}) + B\,(T - T_{\mathrm{ref}})^2}, \tag{2}$$

where ρ_{ref} is the reference density for T_{ref}, A is the linear volumetric expansion coefficient and B is the quadratic

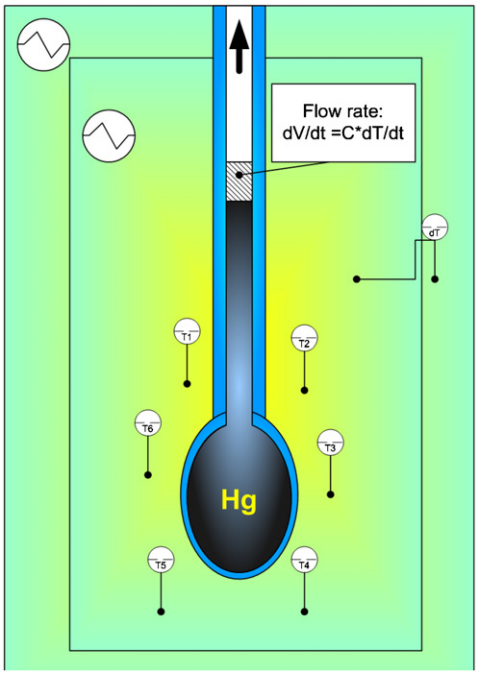

Figure 1. Working principle of the nanoflow generator: temperature gradient ($\mathrm{d}T/\mathrm{d}t$) results in a volume gradient ($\mathrm{d}V/\mathrm{d}t$), hence a fluid flow. The figure shows the mercury reservoir connected to an open capillary and an inner and outer controlled temperature bath.

volumetric expansion coefficient. Combining (1) and (2) yields

$$V(T) = \frac{m}{\rho_{\mathrm{ref}}}(1 + A(T - T_{\mathrm{ref}}) + B(T - T_{\mathrm{ref}})^2). \tag{3}$$

As mentioned before, to demonstrate the proof of principle of the nanoflow generator, we ensure a constant increase of the temperature in time:

$$T(t) = T_0 + kt, \tag{4}$$

where T_0 is the initial temperature, t is the time in seconds and k is the temperature gradient. Combining (3) and (4) yields the volume of mercury as a function of time:

$$V(t) = \frac{m}{\rho_{\mathrm{ref}}}(1 + A(kt + T_0 - T_{\mathrm{ref}}) + B(kt + T_0 - T_{\mathrm{ref}})^2). \tag{5}$$

The derivative of (5) with respect to time yields the flow rate

$$Q(t) = \frac{\partial V(t)}{\partial t} = \frac{mk}{\rho_{\mathrm{ref}}}(A + 2B(kt + T_0 - T_{\mathrm{ref}})). \tag{6}$$

Note that the effective flow rate will also depend on the dilatation of the glass. However, because the volumetric thermal expansion of glass is almost an order of magnitude smaller than the volumetric expansion of mercury, the flow rate due to the dilatation of glass is initially neglected. Future work will include the effect of the glass dilatation on the flow rate. Finally, the expansion of mercury due to the quadratic term in temperature can also be neglected for the temperature range that we consider (around room temperature). Hence, (6) can be simplified to

$$Q = \frac{mkA}{\rho_{\mathrm{ref}}}. \tag{7}$$

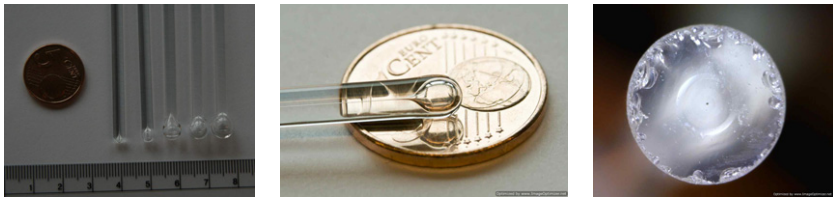

(*a*) (*b*) (*c*)

Figure 2. Prototype of the nanoflow generator as developed by VSL. (*a*) Various nanoflow generators with different reservoirs but same capillary diameter. (*b*) Relative size of the nanoflow generator. (*c*) Cross section of the nanoflow generator showing capillary.

In section 4 we show that this simple theoretical model is sufficient to predict the flow rate. The design operating conditions for the nanoflow generator are $m = 0.034$ g, $k = 0.0024\,^{\circ}\mathrm{C\ s^{-1}}$, $A = 1.81 \times 10^{-4}\,^{\circ}\mathrm{C^{-1}}$ and $\rho_{\mathrm{ref}} = 1.355 \times 10^{-2}\,\mathrm{g\,mm^{-3}}$. This leads to a generated flow rate of $1.09 \times 10^{-3}\,\mathrm{nl\,s^{-1}}$ (nanoliters per second).

Since the mercury is used to drive another fluid, the net flow rate of the fluid of interest is also affected by the temperature gradient. However, in this proof of principle we will only consider the flow rate of mercury. Future work will include investigations into the expansion of the fluid of interest. Since the temperature gradient is accurately known, the expansion of the fluid of interest can relatively easily be corrected for. In future work we may also consider fixing the temperature of the fluid of interest at a constant value, or using more than one driver fluid with a relatively small volumetric expansion coefficient for the fluid that is in contact with the fluid of interest.

2.3. Realization of the prototype

We found a laboratory glassblower able to create the nanoflow generator on the basis of a specified volume of the reservoir. In figure 2(*a*) five different nanoflow generators are shown; from left to right the reservoirs contain approximately 0.034 83 g, 0.161 g, 1.064 g and 1.42 g mercury. The outer diameter of the glass bar capillary is 4.0 mm and the diameter of the capillary is approximately 5.1×10^{-2} mm. Figure 2(*b*) gives an idea of the relative size of the smallest nanoflow generator, whereas figure 2(*c*) gives an idea of the dimensions of the capillary; note the small black dot of mercury in the center of the magnified cross section of the nanoflow generator.

In order to fill the nanoflow generators with mercury, the nanoflow generators are evacuated and then placed upside down in a bath of mercury. The net mass of mercury is obtained by weighing the nanoflow generator before and after the filling procedure. Note that because the mercury in the nanoflow generator is exposed to the open air, some of the mercury will evaporate. However, according to [11] the evaporation of a drop of mercury of 0.2 g is approximately $1.5 \times 10^{-6}\,\mathrm{g\,h^{-1}}$ at room temperature, which compares to an evaporation rate of $3.1 \times 10^{-8}\,\mathrm{nl\,s^{-1}}$, which is only 0.0028% of the design flow rate. Furthermore, because of the very small diameter of the capillary (5.1×10^{-2} mm), only a fraction of the total mercury is exposed to the open air, which results in an even smaller evaporation rate. Hence, it is safe to neglect the evaporation of mercury.

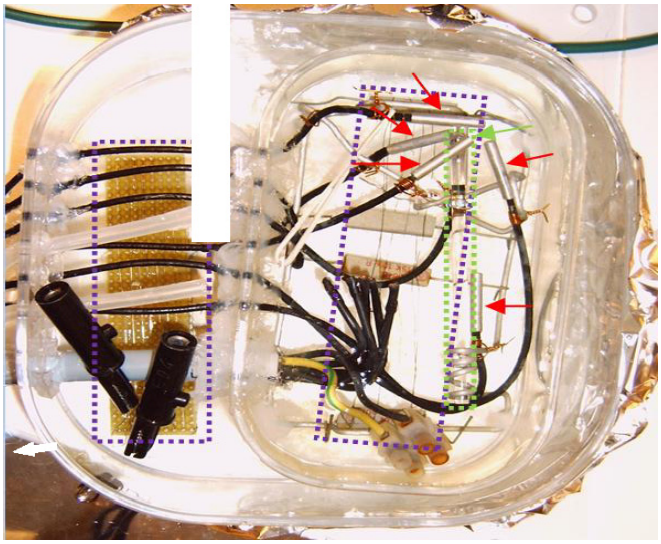

Figure 3. Nanoflow generator and controlled dynamic temperature bath. Dots in the larger rectangles (purple) indicate the resistor bridges, dots in the smallest rectangle (green) indicate the outside glass bar containing the capillary, arrows (red) point to the temperature sensors, except for the upper right arrow (green), which points to the mercury reservoir.

The complete setup is shown in figure 3. One can distinguish outer and inner thermodynamic temperature baths which are heated by straightforward resistor bridges. The arrows point to six NTC temperature sensors and the mercury reservoir (green arrow at upper right). The smallest dotted rectangle (green) indicates the outside of the glass bar and its capillary outlet which is just above the water level.

The complete setup is placed in a temperature controlled laboratory to further minimize heat leakage. In order to be able to verify the constant temperature increase the water bath is equipped with six NTC temperature sensors with a resolution of 1 mK. We note that there may be a temperature difference between the mercury and the water. However, this is not a problem as long as the temperature of the mercury increases constantly in time. Furthermore, we anticipate very little temperature difference because the temperature in the water bath is very gradually increased.

3. Rangeability and uncertainty

In this section the uncertainty and rangeability are, respectively, discussed.

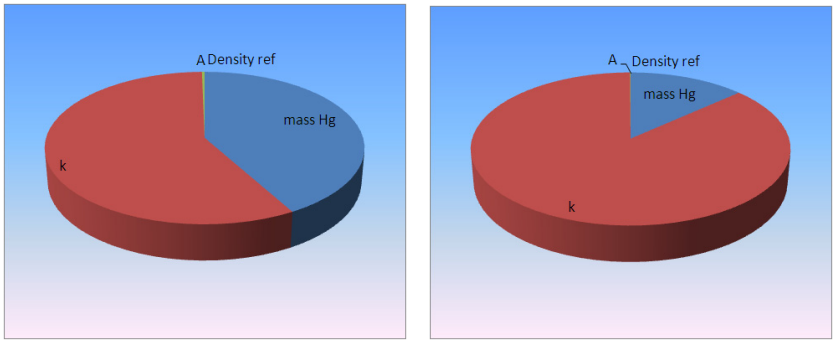

(*a*) (*b*)

Figure 4. Uncertainty balance for a nanoflow rate of 1.09×10^{-3} nl s^{-1}. (*a*) Mercury mass is 3.4×10^{-2} g. (*b*) Mercury mass is 5.0×10^{-2} g.

Table 1. Estimated uncertainty in flow rate due to the uncertainties in operating conditions: ux is the estimated uncertainty, 'sens.' is the sensitivity of the nanoflow with respect to the uncertain parameter, 'ux in Q' is the estimated uncertainty in nanoflow rate. The first column gives the design operating conditions, the last column gives the relative uncertainty in the flow rate.

Parameter	Value	Unit	ux (2 s)	sens.	ux in Q	Uncertainty (%)
mass Hg	0.034	g	4.00×10^{-5}	3.21×10^{-5}	1.28×10^{-9}	0.118
k	0.0024	°C s^{-1}	3.32×10^{-6}	4.54×10^{-4}	1.51×10^{-9}	0.139
A	1.81×10^{-4}	°C^{-1}	1.81×10^{-8}	6.02×10^{-3}	1.09×10^{-11}	<0.1
ρ_{ref}	1.3546×10^{-2}	g mm^{-3}	2.00×10^{-5}	1.48×10^{-8}	2.80×10^{-13}	<0.1

3.1. Uncertainty

In this section the uncertainty of the generated nanoflow rate is evaluated according to the recommended procedure in [12]. According to (7), the relevant parameters with respect to the uncertainty in the flow rate are the mass of mercury (m), the temperature gradient (k), the expansion factor of mercury (A) and the reference density (ρ_{ref}). These uncertainties and their influence on the flow rate are discussed in the following subsections.

3.1.1. Uncertainty in the mercury mass. The uncertainty in the mercury mass (Δm_{Hg}) is 4.0×10^{-5} g and is due to the used differential mass determination of an empty and filled capillary reservoir combination.

3.1.2. Uncertainty in the temperature gradient. The anticipated uncertainty in the temperature gradient is due to the noise of the temperature sensors and nonlinear effects. The uncertainty in the temperature gradient (Δk) is estimated at 3.32×10^{-6} °C s^{-1} and is based on an uncertainty analysis of the average slope of the dynamic temperature sensors around the mercury reservoir, see section 4.1.

3.1.3. Uncertainty in the material properties of mercury. The uncertainty in A (ΔA) is 1.81×10^{-8} °C^{-1}, see [10]. The uncertainty in the reference density ($\Delta \rho_{\text{ref}}$) is 2.0×10^{-5} g mm^{-3}, see [10].

3.1.4. Uncertainty in the flow rate. Next, the influence of these uncertainties on the flow rate is determined. The sensitivity of the flow rate is determined by the partial derivatives of (7) with respect to the uncertain parameter. The influence of the uncertainty on the flow rate is the product of the sensitivity and the uncertainty. For example, the sensitivity of the flow rate with respect to the mass of mercury is

$$\frac{\partial Q(t)}{\partial m_{\text{Hg}}} = \frac{kA}{\rho_{\text{ref}}}. \tag{8}$$

The influence of the uncertainty in the mass of mercury on the flow rate is, therefore,

$$\frac{\partial Q(t)}{\partial m_{\text{Hg}}} \Delta m_{\text{Hg}} = \frac{kA}{\rho_{\text{ref}}} \Delta m_{\text{Hg}}. \tag{9}$$

In table 1 the uncertainty, the sensitivity and the uncertainty in the flow rate are given for the aforementioned parameters. As expected, the mass of mercury and the temperature gradient have the largest impact on the uncertainty in the generated nanoflow. However, table 1 clearly reveals that the impact of the various uncertainties on the flow rate is rather small, i.e. of the order of 0.1% and lower. This implies that the generated nanoflow is known with a very small uncertainty. For mercury masses of 34 mg and 50 mg the uncertainty balance is given in figure 4.

3.2. Rangeability

According to (7) the flow rate range of the nanoflow generator depends on the mercury mass, the temperature gradient, the thermal expansion coefficient of mercury and the reference density. Since the latter two are material properties they cannot be modified. Hence, there are two approaches to adjust the flow rate of the nanoflow generator:

- adjusting the mercury mass;
- adjusting the dynamic temperature slope.

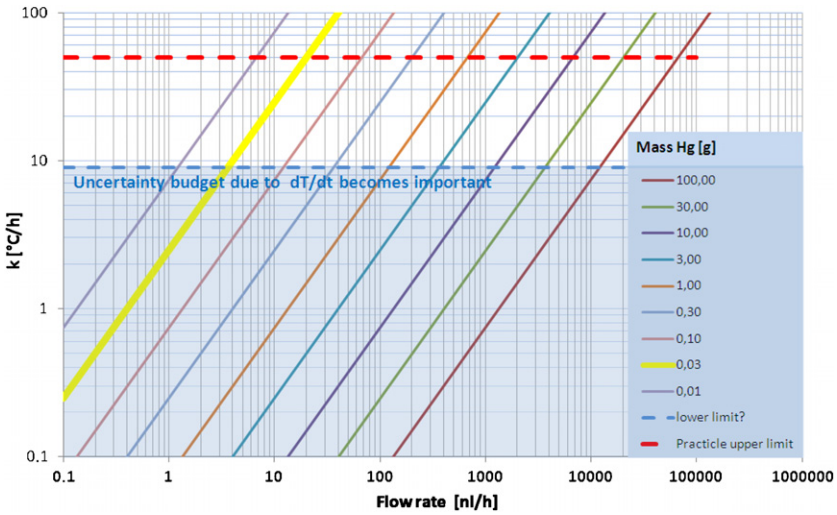

Figure 5. Rangeability of the nanoflow generator. The solid lines from left to right are for increasing mercury mass (mass Hg).

Adjusting the mercury mass is not easy because each nanoflow generator can only contain a certain amount of mercury. The minimum mass of mercury is also limited to the uncertainty level that can be achieved with the determination of the mass. For example, the uncertainty for mass determination at VSL for this application is 4×10^{-5} g (2σ). Because the smallest reservoir contains 0.034 g, the uncertainty starts to dominate for even smaller reservoirs. Obviously, there is also a maximum in order to avoid overflowing. Hence, in order to adjust the flow rate by means of adjusting the mass of mercury, one has to use a different reservoir and possibly a different capillary.

The flow rate can also be adjusted by modifying the temperature gradient. A larger temperature gradient results in a larger flow rate. The maximum total volume flow, however, remains limited to the length of the capillary. In figure 5 the range of the nanoflow generator is given as a function of the temperature gradient (k) and mercury mass (mass Hg). The solid lines represent a flow rate for a certain temperature gradient and mercury mass. The area between the dashed lines indicates the range in which the nanoflow generator has low uncertainty and is practical to apply.

4. Results

In this section the results obtained with the nanoflow generator prototype are discussed. The goal of this section is to validate the proof of principle claimed in the introduction. This is accomplished by demonstrating a constant temperature gradient and a constant flow rate in the next two sections, respectively.

4.1. Constant temperature gradient

In order to determine the temperature gradient of the mercury the reservoir is closely surrounded by five temperature sensors (numbers 1, 2, 3, 4 and 6), whereas sensor number 5 is placed a few centimeters away from the reservoir (see figure 3 for the location of the various sensors, sensor number 5 is indicated by the bottom arrow). In figure 6(a) the temperature as a function of time and for the various temperature sensors is shown. Following a least-squares approach a constant temperature gradient is determined to be $0.0015\,^{\circ}\mathrm{C\,s^{-1}} = 5.4\,^{\circ}\mathrm{C\,h^{-1}}$ (slightly lower than the design operating conditions).

Figure 6(b) shows the error made with respect to the assumed constant temperature gradient. According to figure 6(b) the largest error made is 5×10^{-3} °C. Following the recommendations taken from ISO/DIS 7066-1.2 [13], this error amounts to an uncertainty of 3.32×10^{-6} $^{\circ}\mathrm{C\,s^{-1}}$ (2 times standard deviation).

4.2. Constant flow rate

Due to the lack of flowmeters in the nanoflow regime, the nanoflow generator cannot yet be compared with other systems by means of a calibration with a 'traveling meter'. Therefore, we have measured the mercury level as a function of time in order to verify whether the theoretical flow rate is achieved. These results are only qualitative because of a rather large uncertainty in the diameter of the capillary (approximately 10%). However, when it is assumed that the capillary has a constant diameter (fair assumption based on the specifications of the laboratory glassblower), a constant velocity of the mercury level demonstrates a constant flow rate.

The results discussed next are obtained for a flow rate of 1.65×10^{-2} nl s^{-1} which is achieved with $m_{\mathrm{Hg}} = 1.064$ g, $A = 1.81 \times 10^{-4}\,^{\circ}\mathrm{C}^{-1}$, $\rho_{\mathrm{ref}} = 1.355 \times 10^{-2}\,\mathrm{g\,mm^{-3}}$ and $k = 0.001\,16\ ^{\circ}\mathrm{C\,s^{-1}}$. In a similar way as discussed in section 3.1, the uncertainty in the flow rate is determined to be 3.61×10^{-5} nl s^{-1}.

In order to measure the mercury level as a function of time we use microscope readings, illustrated in figure 7. This figure shows two recordings of the level of the mercury (indicated by the arrow). We define the zero-level for a zero length of the arrow in figure 7. Next, figure 8(a) shows the traversed length of the mercury level. Figure 8(b) shows the residual when

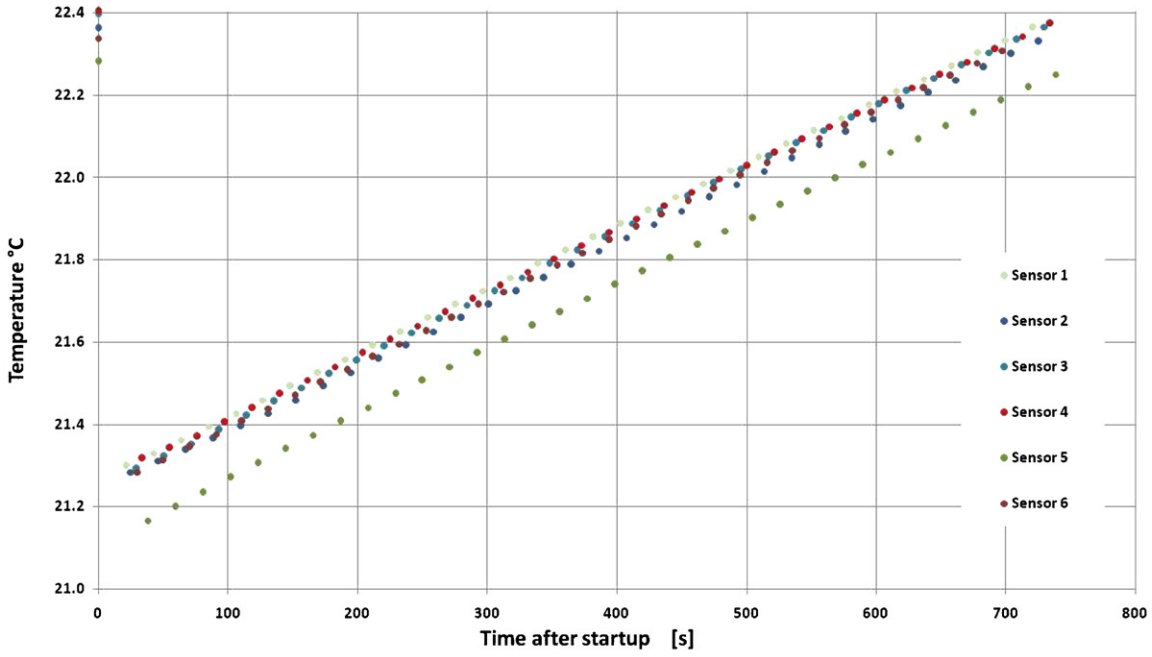

(*a*)

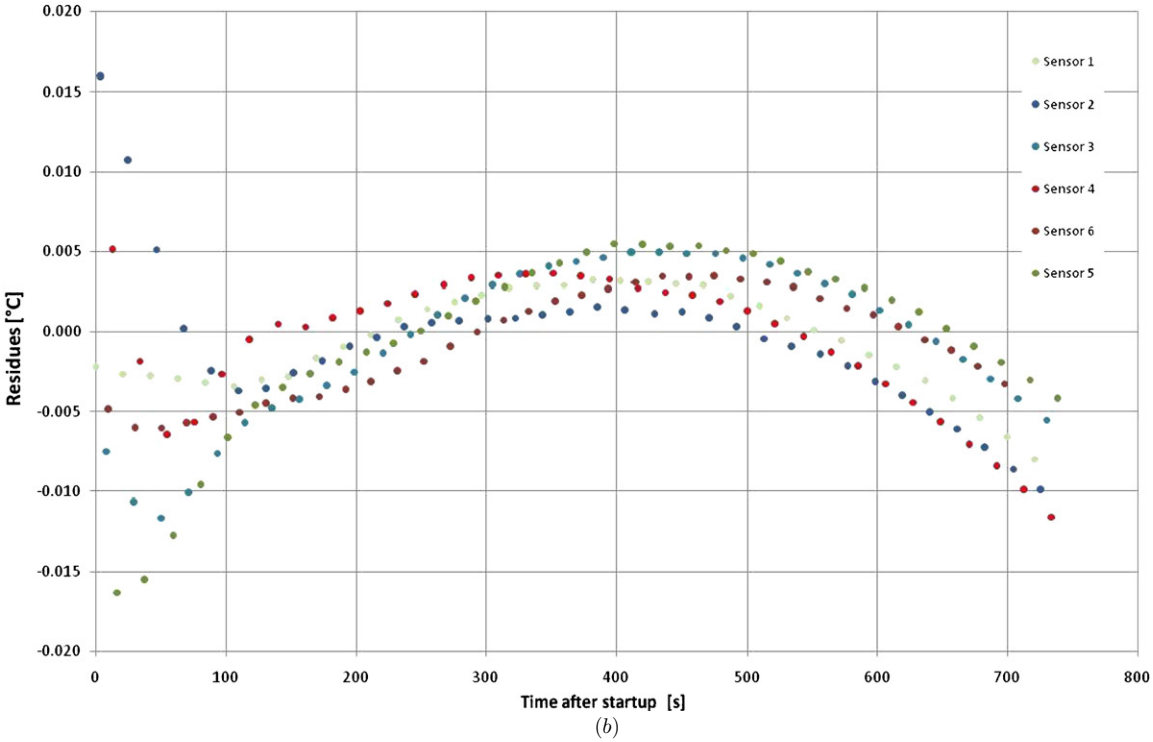

(*b*)

Figure 6. Dynamic temperature of the water bath. (*a*) Temperature of the water bath according to the various thermometers. (*b*) Residual for the assumption of a constant temperature gradient.

a constant expansion in time is assumed. From figure 8(*b*) it follows that the assumption of a constant expansion is accurate to 0.10 mm (maximum relative error is approximately 3%). Hence, from figure 8 it can be concluded that the expansion of the mercury is virtually constant in time, thus generating a constant flow rate. From figure 8(*a*) the flow rate can be deduced with

$$Q_{\text{measured}} = \frac{\Delta L}{\Delta t}\pi r^2_{\text{capillary}}. \tag{10}$$

Filling in the unknowns in (10) yields a flow rate of 1.53×10^{-2} nl s^{-1}. Compared to the predicted flow rate of 1.65×10^{-2} nl s^{-1} this yields an error of 7.84%. This mismatch between the theoretical and the observed flow rate is due to the uncertainty in the capillary diameter (10%).

Note that the relatively large mismatch between the observed and the theoretical flow rates does not mean a large uncertainty in the flow rate. The uncertainty in the flow rate (type B) is related to the mercury mass, temperature gradient,

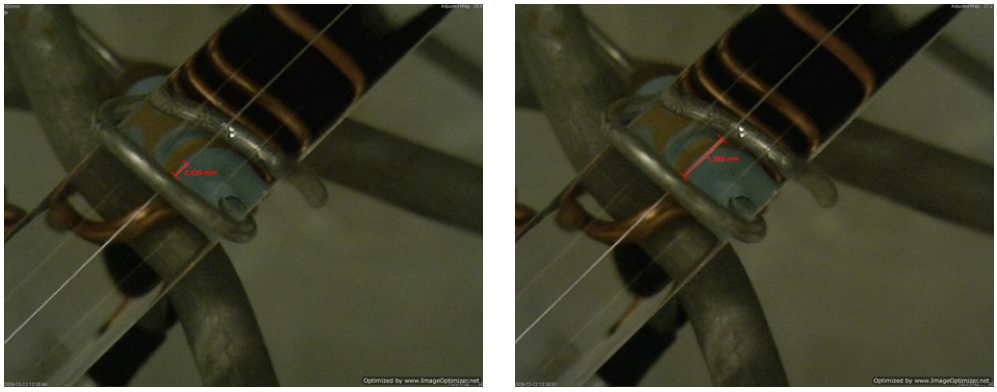

(*a*) (*b*)

Figure 7. Two measurements of the mercury level. The arrow indicates relative traversed distance of the mercury level. (*a*) Mercury level at a certain position in time. (*b*) Mercury level at the next position in time.

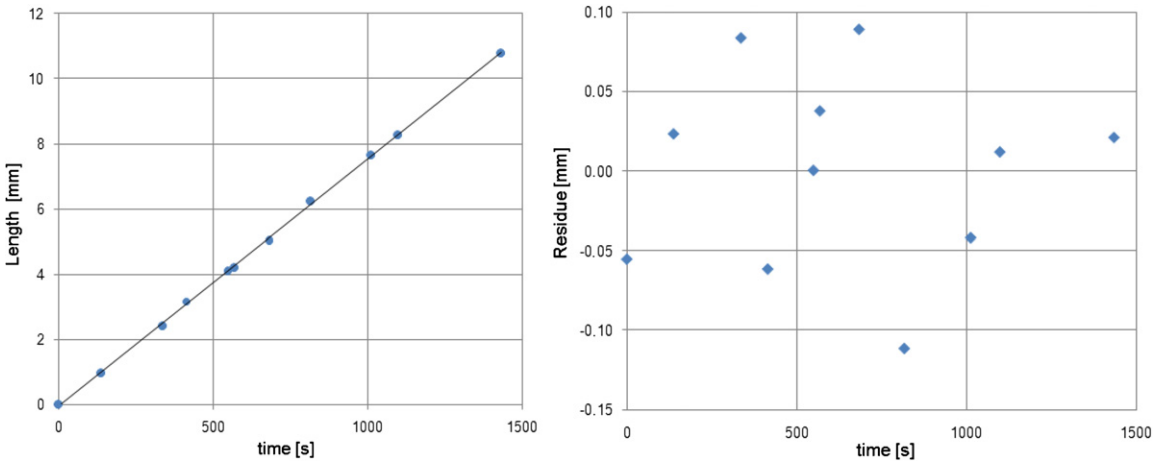

(*a*) (*b*)

Figure 8. (*a*) Level of the mercury and (*b*) residual with respect to an assumed constant expansion of mercury.

mercury expansion coefficient and mercury reference density. The uncertainty in the flow rate is, however, not related to the diameter of the capillary because the flow rate does not depend on it. The observed 'flow rate' is, however, obviously related to the capillary diameter.

5. Conclusions and future work

The goal of the research carried out at VSL is to develop a relatively simple and straightforward to apply primary standard/flowgenerator in the nanoflow regime with a sound traceability and low uncertainty. This paper demonstrated a proof of principle of a nanoflow generator down to a flow rate of 1.09×10^{-3} nl s^{-1}. The nanoflow generator has a straightforward working principle, a sound traceability chain to SI units and a rather small uncertainty. The uncertainty is determined to be approximately 0.1% (2σ), which is mainly caused by the determination of the mass of mercury and the temperature gradient. Comparison with other devices or standards cannot yet be performed; however, a qualitative comparison proved consistency.

VSL has scheduled to develop a small facility to do further research on this topic in 2010–2011. The range will be expanded to flow rates up to 1000 nl min^{-1}. Challenges are to achieve an accurate flow rate of the fluid of interest (temperature gradient in fluid of interest), to get a fast response of the average temperature in larger liquid-reservoirs, to have a bubbly-free operation when working with water on top of the mercury and to avoid linepack issues.

Acknowledgments

The authors would like to thank Tijmen Mateboer who cleared numerous hurdles to make the experiment work, for example traveling by train to Germany with filled capillaries in Thermos bottles to 'keep them cool', Inge van Andel for her expertise on mass and Andrea Peruzzi for his expertise on temperature.

References

[1] Angarra R, Li S and Anjanapapa M 2009 Automated long-term storage and precision microdispensing system for precious biologic solutions *Mechatronics* **19** 878–85

[2] Werner M and Kammerstetter H 2009 The role of metrological traceability of very small injection quantities in the automotive industry *European Meeting on Microflow Metrology (PTB, Braunschweig, Germany)*
[3] Ewart T, Perrier P, Graur I and Méolans J G 2006 Mass flow rate measurements in gas micro flows *Exp. Fluids* **41** 487–98
[4] Jian W and Ann C H 2006 A new primary gas flow standard for flow rate measurements from 0.001 to 1000 NANO mol/s *XVIII IMEKO World Congress (Rio de Janeiro, Brazil)*
[5] Jousten K, Menzer H and Niepraschk R 2002 A new fully automated gas flowmeter at the PTB for flow rates between 10^{-13} mol/s and 10^{-6} mol/s *Metrologia* **39** 519–29
[6] Pitakarnnop J, Varoutis S, Valougeorgis D, Geoffroy S, Baldas L and Colin S 2010 A novel experimental setup for gas microflows *Microfluid Nanofluid* **8** 57–72
[7] Laser D J and Santiago J G 2004 A review of micropumps *J. Micromech. Microeng.* **14** R35–64 (topical review)
[8] Wijshof H 2008 Structure- and fluid-dynamics in pieze inkjet printheads *PhD Thesis* Delft University of Technology, Delft, The Netherlands
[9] van der Beek M P 2009 An experimental primary standard for the nano-flow region *European Meeting on Microflow Metrology (PTB, Braunschweig, Germany)*
[10] Brown I and Lane J E 1976 Recommended reference materials for realization of physicochemical properties, section: density *Pure Appl. Chem.* **45** 1–9
[11] Winter T G 2003 The evaporation of a drop of mercury *Am. J. Phys.* **71** 783–6
[12] International Organization for Standardization (Geneva) 1993 *Guide to the Expression of Uncertainty in Measurement* Online at www.iso.org
[13] International Organization for Standardization (Geneva) 1988 *Assessment of Uncertainty in the Calibration and Use of Flow Measurement Devices, Part I: Linear Calibration Relationships* Online at www.iso.org (ISO 7066-1.2)